

Synergistic Graph Fusion via Encoder Embedding

Cencheng Shen^{*1}, Carey E. Priebe², Jonathan Larson³, and Ha Trinh³

¹Department of Applied Economics and Statistics, University of Delaware

²Department of Applied Mathematics and Statistics, Johns Hopkins University

³Microsoft Research, Redmond

April 3, 2023

Abstract

In this paper, we introduce a novel approach to multi-graph embedding called graph fusion encoder embedding. The method is designed to work with multiple graphs that share a common vertex set. Under the supervised learning setting, we show that the resulting embedding exhibits a surprising yet highly desirable "synergistic effect": for sufficiently large vertex size, the vertex classification accuracy always benefits from additional graphs. We provide a mathematical proof of this effect under the stochastic block model, and identify the necessary and sufficient condition for asymptotically perfect classification. The simulations and real data experiments confirm the superiority of the proposed method, which consistently outperforms recent benchmark methods in classification.

Keywords: Graph Fusion, Encoder Embedding, Vertex Classification, Stochastic Block Model

1 Introduction

Graphs are increasingly prevalent in various real-world scenarios such as social networks, communication networks, webpage hyperlinks, and biological systems [1–6]. The graph data consists of a set of vertices $v_i, i = 1, \dots, n$ and the edges $e_j, j = 1, \dots, s$ between them, which can be represented by an $n \times n$ adjacency matrix A . In practice, most graphs are sparse and are typically stored as an $s \times 3$ edgelist E , where the first two columns indicate the vertex indices of each edge and the last column represents the edge weight.

The graph embedding approach is a fundamental and versatile method for analyzing and exploring graph data, encompassing a broad range of techniques including spectral embedding [7, 8], graph convolutional neural networks [9, 10], node2vec [11, 12],

^{*}shenc@udel.edu

among others. By projecting the vertices into a low-dimensional space while preserving the structural information of the graph, graph embedding produces a vertex representation in Euclidean space that enables various downstream inference tasks, such as community detection [13, 14], vertex classification [9, 15], outlier detection [16, 17], etc.

This manuscript focuses on an increasingly important scenario in which we have multiple graphs with a shared vertex set, which frequently arises in practice when analyzing different social network connections for the same group of individuals, different measurements on the same brain regions, etc. It is also common to transform a single graph dataset into multiple graphs by, for example, converting a weighted graph into a binary graph or generating additional graphs from existing vertex attributes. Naturally, we aim to improve subsequent inference tasks by incorporating additional graphs.

To that end, we introduce a new multi-graph embedding approach called graph fusion encoder embedding, building upon the recently proposed graph encoder embedding [18]. This method is both computationally efficient and straightforward to implement. Its most distinctive feature is what we refer to as the "synergistic effect" in the supervised learning setting, where for sufficiently large vertex size, the vertex classification accuracy never degrades with additional graphs. This unique property ensures that the method is robust against noisy graphs and benefits consistently from additional graphs. We provide a mathematical proof of this effect under the stochastic block model and its degree-corrected variant [13, 19, 20]. Furthermore, we derive the necessary and sufficient condition for the graph fusion encoder embedding to be asymptotically perfect for vertex classification, which further clarifies the synergistic effect. Finally, we provide comprehensive simulations and real graph evaluations to validate the superiority of the method.

The appendix includes all proofs and additional numerical experiments on three recent multiple-graph methods: omnibus embedding (Omnibus) [21, 22], multiple adjacency spectral embedding (MASE) [23], and unfolded spectral embedding (USE) [24]. These comparisons show that the graph fusion encoder embedding significantly outperforms others and is the only method to exhibit the synergistic effect. The MATLAB code for the method and simulations are made available on Github¹.

¹<https://github.com/cshen6/GraphEmd>

2 Method

The graph fusion encoder embedding takes as input M edgelists with a common set of n vertices and a label vector of K communities. For vertices with unknown labels, the corresponding entry in the label vector is set to 0.

- **Input:** The edgelists $\{\mathbf{E}_s \in \mathbb{R}^{s_m \times 3}, m = 1, \dots, M\}$ and a label vector $\mathbf{Y} \in \{0, 1, \dots, K\}^n$.
- **Step 1:** For each $k = 1, \dots, K$, compute the number of observations per-class

$$n_k = \sum_{i=1}^n I(\mathbf{Y}_i = k),$$

for which the unknown labels, i.e., all the zero entries, are unused.

- **Step 2:** Compute the one-hot encoding matrix $\mathbf{W} \in \mathbb{R}^{n \times K}$ for the given label vector \mathbf{Y} , with all zero entries being unused and effectively treated as zero vectors in \mathbf{W} . Then, for each class $k = 1, \dots, K$, normalize the corresponding column of \mathbf{W} using

$$\mathbf{W}(\mathbf{Y} = k, k) = \mathbf{W}(\mathbf{Y} = k, k) / n_k.$$

- **Step 3:** For each graph $m = 1, \dots, M$, calculate

$$\mathbf{Z}_m = \mathbf{A}_m \times \mathbf{W}, \tag{1}$$

where \mathbf{A}_m represents the adjacency matrix of \mathbf{E}_m .

- **Step 4:** Let $\mathbf{Z}_m(i, \cdot)$ denote each row of \mathbf{Z}_m . For each i and each m where $\|\mathbf{Z}_m(i, \cdot)\|_2 > 0$, normalize the non-zero row by its Euclidean norm as follows:

$$\mathbf{Z}_m(i, \cdot) = \frac{\mathbf{Z}_m(i, \cdot)}{\|\mathbf{Z}_m(i, \cdot)\|_2}.$$

- **Step 5:** Form the row-concatenated embedding \mathbf{Z} by

$$\mathbf{Z}(i, \cdot) = [\mathbf{Z}_1(i, \cdot) | \mathbf{Z}_2(i, \cdot) | \dots | \mathbf{Z}_M(i, \cdot)] \in \mathbb{R}^{MK}.$$

for each vertex i .

- **Output:** The graph fusion encoder embedding $\mathbf{Z} \in \mathbb{R}^{n \times MK}$.
- **Classification:** Train a nearest-neighbor classifier $g(\cdot)$ using (\mathbf{Z}, \mathbf{Y}) with known labels.

The computation complexity of the fusion encoder embedding is $O(nMk + \sum_{m=1}^M s_m)$, with a constant overhead of about 2. If $M = 1$, the fusion encoder embedding is equivalent to the normalized encoder embedding for a single graph [18, 25]. While the other steps are straightforward to analyze, step 3, which involves matrix multiplication, can be implemented in linear time using two simple edgelist operations. Furthermore, step 3 can be parallelized across different graph data before concatenation, further reducing the running time to $O(nk + \max_{m=1, \dots, T} s_m)$. Although computation details are not the focus of this paper, previous work [18, 26] has demonstrated that the encoder embedding outperforms existing methods and can process millions of edges in minutes.

The label vector is always available in the supervised setting. The labels of the training vertices are used in step 1 to 3 to construct the W matrix, whereas the label of testing vertices are set to zero and unused throughout the embedding process. Both the training and testing vertices are present in the edgelists, so the final embedding \mathbf{Z} captures the vertex embedding for all vertices.

We denote the classification error by

$$L = \text{Prob}(g(\mathbf{Z}(v, :)) \neq y_v),$$

where y_v is the true label for vertex v , and $g(\cdot)$ denotes the classifier function. Throughout the paper, we use the 5-nearest-neighbor classifier, which is sufficient for the asymptotic theory and performs well in experiments. Other classifiers such as discriminant analysis, random forest, or a simple two-layer neural network can be used to obtain similar numerical results.

3 Theory

The theory and simulations of the paper focus on the stochastic block model (SBM), so we provide a brief overview. For a given graph \mathbf{A}_m , with $m = 1, \dots, M$, each vertex i is assigned a label $Y_i \in \{1, \dots, K\}$ based on a categorical distribution with prior probability $\pi_k \in (0, 1)$ with $\sum_{k=1}^K \pi_k = 1$. The probability of an edge between a vertex from class k and a vertex from class l is determined by a block probability matrix $\mathbf{B}_m = [\mathbf{B}_m(k, l)] \in$

$[0, 1]^{K \times K}$, and for any $i < j$ it holds that

$$\begin{aligned}\mathbf{A}_m(i, j) &\stackrel{i.i.d.}{\sim} \text{Bernoulli}(\mathbf{B}_m(Y_i, Y_j)), \\ \mathbf{A}_m(i, i) &= 0, \quad \mathbf{A}_m(j, i) = \mathbf{A}_m(i, j).\end{aligned}$$

The degree-corrected stochastic block model (DC-SBM) is an extension of the SBM that accounts for the sparsity of real graphs [14]. In addition to the parameters defined in the SBM, each vertex i is given a degree parameter θ_i , and the adjacency matrix is generated by

$$\mathbf{A}_m(i, j) \sim \text{Bernoulli}(\theta_i \theta_j \mathbf{B}_m(Y_i, Y_j)).$$

To ensure a valid probability, the degree parameters are usually constrained. In this paper, we assume that the degree parameters are non-trivial, bounded, and independently distributed, i.e., $\theta_i \stackrel{i.i.d.}{\sim} F\theta$.

Given M SBM graphs with a common vertex set, we denote $\mathbf{B} \in \mathbb{R}^{K \times MK}$ as the row-concatenated block probability matrix of all \mathbf{B}_m . Moreover, we define $\tilde{\mathbf{B}}_m$ as the row-normalized block probability matrix of \mathbf{B}_m , such that for each row k ,

$$\tilde{\mathbf{B}}_m(k, :) = \frac{\mathbf{B}_m(k, :)}{\|\mathbf{B}_m(k, :)\|_2}.$$

We denote the row concatenation of all $\tilde{\mathbf{B}}_m$ as $\tilde{\mathbf{B}} \in \mathbb{R}^{K \times MK}$.

The first theorem establishes the convergence of the graph fusion encoder embedding, which is a direct consequence of the convergence theorem in [18] applied to a normalized and concatenated embedding.

Theorem 1 (Asymptotic Convergence). *Suppose that each graph \mathbf{A}_m follows a DC-SBM model with a block probability matrix \mathbf{B}_m for $m = 1, \dots, M$. Let n be the number of vertices with known labels. Then, for any vertex i belonging to class y , the fusion encoder embedding satisfies:*

$$\|\mathbf{Z}(i, \cdot) - \tilde{\mathbf{B}}(y, :)\|_2 \xrightarrow{n \rightarrow \infty} 0.$$

The next theorem proves the necessary and sufficient condition for the graph fusion encoder method to be asymptotically perfect for vertex classification.

Theorem 2 (Asymptotic Perfect Separation). *Assuming that the training and testing vertices follow the same distribution, and in the same setting as Theorem 1, the graph fusion*

encoder method achieves asymptotically perfect classification, i.e.,

$$L \xrightarrow{n \rightarrow \infty} 0,$$

if and only if there are no repeating rows in $\tilde{\mathbf{B}}$, or equivalently, no repeating rows up to multiplication in \mathbf{B} .

In essence, the graph fusion encoder method can achieve perfect classification when there is no overlap between the rows of $\tilde{\mathbf{B}}$, meaning that each row represents a unique class. Conversely, if any two rows of $\tilde{\mathbf{B}}$ coincide, then the embedding vectors for vertices in those two classes will also coincide, making them indistinguishable.

Next we describe the synergistic effect of the embedding.

Theorem 3 (Synergistic Effect). *Assume the same setting as Theorem 2, and given two finite sets of graphs \mathbf{G}_1 and \mathbf{G}_2 where $\mathbf{G}_1 \subseteq \mathbf{G}_2$ and every graph in the sets shares a common vertex set. The graph fusion encoder method using nearest-neighbor classifier satisfies*

$$L_{\mathbf{G}_2} \leq L_{\mathbf{G}_1}$$

for sufficiently large number n .

This synergistic effect theorem states that the graph fusion encoder method can only improve its classification error (equal or better) as more graphs are included in the input. Even when noise graphs are added, the classification error does not deteriorate. Moreover, the additional graphs may contain useful information for certain inseparable classes, leading to a reduction in classification error.

It is important to note that since the theorems are based on asymptotic results, there is a possibility of minimal deterioration in the finite-sample error, particularly for small vertex sizes. Moreover, while existing graphs may already be asymptotically perfect for classification, adding more graphs could potentially enhance the separability of the block structure and yields better finite-sample error.

4 Simulations

In this section we consider three simulations to provide numerical examples to the theorems and to illustrate the synergistic effect.

Simulation 1

We let $K = 4$ and the prior probability be $[0, 3, 0.2, 0.2, 0.3]$. Three SBM graphs are generated with block probability matrices $B_j \in \mathbb{R}^{K \times K}$. For each j , the probabilities are $B_j(k, l) = 0.1$ for all k, l , except $B_j(j, j) = 0.2$ for $j = 1, 2, 3$. This means that the j th class has a stronger connection in graph j . A visualization of this setup is provided in Figure 1. While no single graph is asymptotically perfect for classification, the concatenated block probability matrix

$$\mathbf{B} = \begin{bmatrix} 0.2 & \cdots & 0.1 & 0.1 & \cdots & 0.1 & 0.1 & 0.1 & \cdots \\ 0.1 & \cdots & 0.1 & 0.2 & \cdots & 0.1 & 0.1 & 0.1 & \cdots \\ 0.1 & \cdots & 0.1 & 0.1 & \cdots & 0.1 & 0.1 & 0.2 & \cdots \\ 0.1 & \cdots & 0.1 & 0.1 & \cdots & 0.1 & 0.1 & 0.1 & \cdots \end{bmatrix}$$

satisfies the condition in Theorem 2. Therefore, each graph provides additional information to aid in separating the communities, and using all three graphs leads to asymptotic perfect classification.

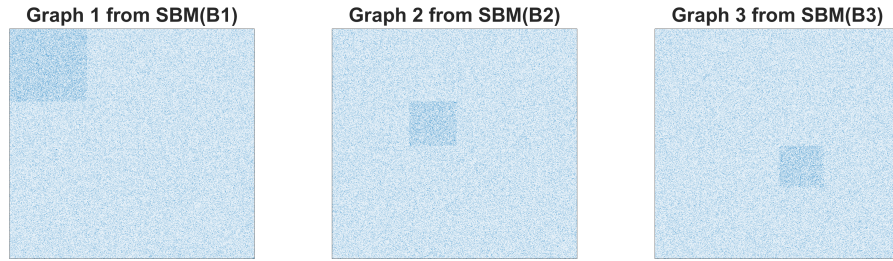


Figure 1: Visualize three SBM graphs at $n = 1000$.

Simulation 2

Simulation 2 uses the same settings as simulation 1, except that the three graphs are generated using DC-SBM. The parameters are the same as above, and the degree parameters are drawn independently from a uniform distribution in the interval $[0.1, 0.5]$.

Simulation 3

This simulation involves starting with one signal graph and progressively adding independent graphs. The number of classes remains at four with the same prior probability. We first

generate \mathbf{A}_1 using SBM with the block probability matrix \mathbf{B}_1 , which has 0.1 in off-diagonal entries and 0.2 in diagonal entries. Next, we generate five independent SBM graphs \mathbf{A}_m for $m = 2, \dots, 6$ with the block probability matrix \mathbf{B}_m being 0.1 in all entries. The concatenated block probability matrix \mathbf{B} always satisfies Theorem 2, even in the presence of independent graphs, i.e.,

$$\mathbf{B} = \begin{bmatrix} 0.2 & 0.1 & 0.1 & 0.1 & \cdots \\ 0.1 & 0.2 & 0.1 & 0.1 & \cdots \\ 0.1 & 0.1 & 0.2 & 0.1 & \cdots \\ 0.1 & 0.1 & 0.1 & 0.2 & \cdots \end{bmatrix}$$

Theorems 2 and 3 predict that the classification error should stay almost the same with the addition of noisy graphs.

Results

The classification error improves with the addition of more graphs in both simulation 1 and simulation 2, as shown in Figure 2, where a 5-nearest-neighbor classifier is used. Using all available graphs yields the lowest error. The errors converge to zero as the vertex size increases, although the convergence is slower in the DC-SBM setting. Adding noise graphs has a negligible effect on the classification error as the number of vertices increases.

The appendix presents the same simulations for three competing methods: Omnibus, MASE, and USE. In both simulation 1 and simulation 2, all three methods were able to enhance the performance, with USE being the best among the three and showing similar results to the fusion encoder embedding. However, in simulation 3, where noise graphs were introduced, all three methods exhibited significant degradation in classification error.

5 Real Data

This section highlights the excellent performance and synergistic effect of the graph encoder embedding using a variety of labeled real graphs. The data used includes graphs that are naturally multi-graph, weighted or directed, or have vertex attributes that can be transformed into a similarity matrix. Most of the data were obtained from the network repository [27], with a few collected by the authors. All the public data has been formatted

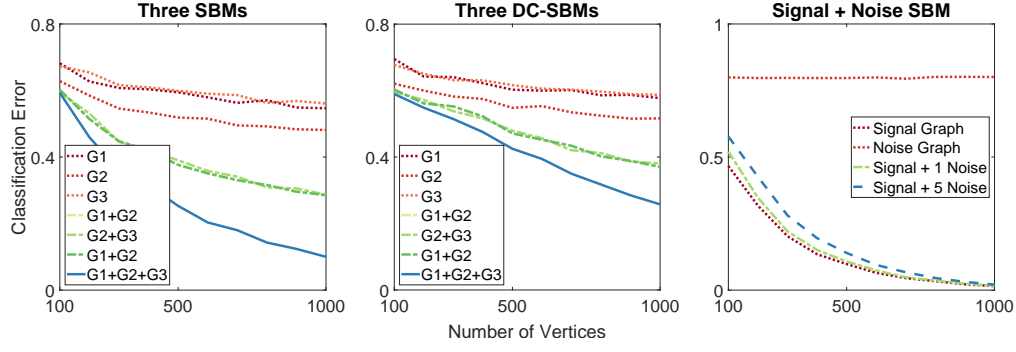


Figure 2: The figure shows the 10-fold classification error of multiple graph fusion, averaged over 20 Monte-Carlo replicates.

in MATLAB and is available on Github². The main paper only presents results for the fusion encoder embedding, while results for Omnibus, MASE, and USE can be found in the Appendix.

5.1 Two-Graph Data

Table 1 presents the 5-fold classification error for seven graph datasets, each having two graphs. The results are reported as the mean and standard deviation over 20 Monte-Carlo replicates. A brief description of each data and pre-processing steps is as follows:

- The C-elegans neuron data [28, 29] consists of two graphs with 253 vertices, over 1000 edges, and a label vector with three classes.
- The cora dataset [30] is a citation network with 2708 vertices and 5429 edges and 7 classes, and each vertex has a 1433-dimensional 0/1 vertex attribute, indicating the absence or presence of corresponding words from the dictionary. We compute the pairwise cosine distance matrix D and transform it by $1 - D$ entrywise into a similarity matrix to form the second graph.
- The citeseer data [31] is another citation network with 3312 vertices and 4715 edges and 6 classes, with a vertex attribute of 3703 dimensions, which is treated similarly as in the cora dataset to form the second graph.
- The IMDB [32] data consists of two graphs, one with binary labels and 19773 vertices, and another with three-class labels and 19502 vertices. We remove the 271

²<https://github.com/cshen6/GraphEmd>

unmatched vertices to ensure a common vertex set, and use the 3-class label as the label vector.

- The protein data [33] has 43471 vertices with 160,000 edges, three classes, and a vertex attribute of 29 dimensions. We compute the pairwise Euclidean distance matrix D and transform it by $1 - D$ entrywise into a similarity matrix to form the second graph.
- COIL-RAG has 11757 vertices with 23588 edges, 100 classes, and a vertex attribute of 64 dimensions, which is treated similarly as in the protein dataset to form the second graph.
- The smartphone dataset has 1703 vertices with 13528 weighted edges, and the second graph is formed by transforming the weight to binary. The label vector has 71 classes based on the phone manufacturer.

In the cora and citeseer datasets, we use the cosine distance computation because it is commonly used in word-frequency analysis [34]. Moreover, we transform the distance matrix into a similarity matrix by subtracting the distance entries from 1, which produces a valid kernel or similarity matrix [35], similar to a dense graph.

The comparison of Table 1 to the tables in Appendix for Omnibus, MASE, and USE reveals that the fusion encoder embedding significantly outperforms all other methods by a large margin across all real data, regardless of whether it is single graph classification or multi-graph classification. The only exception is the C-elegans data where the encoder embedding performs slightly worse, likely due to its small vertex size. Furthermore, the fusion encoder embedding consistently shows improved classification performance as more graphs are included, whereas other methods may exhibit worse errors as more graphs are added, similar to their performance in simulation 3.

5.2 Three-Graph Letter Data

The letter dataset consists of three graphs, named letter-high, letter-med, and letter-low, each of which has its own label vector with a total of 15 classes. The graphs contain over 10500 vertices and 20250, 14092 and 14426 edges, respectively. After removing a few unmatched vertices, we use all three graphs to predict the class labels, and the results are shown in Table 2. The results show that the fusion encoder embedding consistently

	Graph 1	Graph 2	Graph 1+2
C-elegans	42.1% \pm 2.3%	44.5% \pm 3.0%	38.3% \pm 2.4%
Cora	19.2% \pm 0.52%	29.7% \pm 0.48%	15.8% \pm 0.46%
Citeseer	32.3% \pm 0.65%	31.1% \pm 0.45%	27.1% \pm 0.34%
COIL-RAG	7.44% \pm 0.41%	48.4% \pm 0.026%	3.72% \pm 0.24%
IMDB	0.2% \pm 0.03%	0.02% \pm 0.01%	0% \pm 0%
Phone	25.1% \pm 0.68%	24.2% \pm 0.75%	24.0% \pm 0.66%
Protein	32.5% \pm 0.81%	24.9% \pm 0.08%	16.3% \pm 0.04%

Table 1: Evaluate the classification errors using fusion encoder embedding. We report the average 5-fold errors and the standard deviation over 20 Monte-Carlo replicates.

exhibits the synergistic effect. Specifically, the classification error for each graph and its corresponding label is better than that of a mismatched pair, for example using Letter-High to predict Label-High results in better error than using Letter-Mid for the same task. Additionally, using all three graphs yields the best classification error in all cases.

	Letter-High	Letter-Med	Letter-Low	All Graphs
Label-High	3.55% \pm 0.23%	37.1% \pm 0.31%	37.5% \pm 0.25%	3.45% \pm 0.12%
Label-Med	37.7% \pm 0.36%	7.29% \pm 0.25%	37.0% \pm 0.29%	6.13% \pm 0.19%
Label-Low	38.6% \pm 0.26%	38.1% \pm 0.22%	7.12% \pm 0.29%	6.16% \pm 0.23%

Table 2: Evaluate the classification errors using fusion encoder embedding for a three-graph three-label data.

5.3 Four-Graph Wikipedia Data

The Wikipedia dataset consists of four graphs we collected from Wikipedia articles [36, 37]. The datasets has a total of $n = 1382$ Wikipedia articles based on a 2-neighborhood of the English article “Algebraic Geometry” and the corresponding French articles. The hyperlinks in English and French form two separate graphs, while Latent Dirichlet Allocation and

cosine distance are applied to the word-frequency to calculate two other distance matrices named English text and French text. The similarity matrices are then formed using $1 - D$ entrywise. All articles are manually labeled into $K = 5$ disjoint classes: category, people, locations, date, math.

Table 3 displays the classification errors using 5-nearest-neighbor on fusion encoder embedding for the Wikipedia dataset, which demonstrates the synergistic effect. The best error is obtained when all four graphs are utilized, which is slightly better than using only the two text graphs. This indicates that the hyperlink information does not add much signal over the text information in predicting the given labels. Additionally, comparing to the tables in the appendix, the fusion encoder embedding consistently outperforms the other methods in actual classification error and is the only method that exhibits the synergistic effect.

	English Text	French Text	English Hyperlinks	French Hyperlinks
G_1	$19.3\% \pm 0.5\%$	$18.5\% \pm 0.5\%$	$48.6\% \pm 0.9\%$	$52.9\% \pm 1.2\%$
G_2	$16.2\% \pm 0.5\%$ (1+2)	$18.4\% \pm 0.6\%$ (2+4)	$19.0\% \pm 0.5\%$ (1+3)	$44.7\% \pm 1.0\%$ (3+4)
G_3	$16.2\% \pm 0.5\%$ (-4)	$16.1\% \pm 0.5\%$ (-3)	$18.8\% \pm 0.5\%$ (-2)	$18.4\% \pm 0.5\%$ (-1)
G_4	$16.0\% \pm 0.5\%$			

Table 3: Evaluate the classification errors using fusion encoder embedding for a four-graph Wikipedia data. The row of G_1 means the embedding of each individual graph; the row of G_2 means the embedding of using two graphs, e.g., 1+2 means English text + hyperlinks; the row of G_3 means the embedding of using three graphs, e.g., -4 means all graphs excluding French hyperlinks; the row of G_4 is using all graphs.

6 Discussion

This paper presented a graph fusion method via concatenated encoder embedding, and provided compelling evidence on its theoretical soundness and numerical advantages. The most important feature of this method is the synergistic effect, which results in improved numerical performance as more graphs are used regardless of whether they are signal or noise graphs. To some extent, the method can be viewed as a supervised,

edgelist-based, and deterministic version of spectral embedding, but without requiring any additional transformation. In contrast, most competitor methods require extra alignment or additional singular value decomposition.

This paper motivates future research in several areas. Firstly, while this manuscript focuses on a supervised setting, the unsupervised and semi-supervised cases are also worth further consideration. In the absence of labels, the embedding can still be computed, either via some fast labeling methods such as Leiden and label propagation[38–40], or starting with a random label and refining iteratively [25]. However, the subsequent use-case and evaluation is less clear, especially in the unsupervised setting. Secondly, for large values of K or M , the concatenated embedding may have high dimensionality, and it would be interesting to explore dimensionality reduction techniques in this case. Thirdly, the experiments in this paper include the use of graph-like similarity matrices, and the encoder embedding performed surprisingly well, implying its applicability to distance and kernel matrices, which warrants further investigation.

Finally, the synergistic effect is a highly desirable property for graph fusion, and it provides an important criterion for evaluating the quality of multi-graph methods. From the real data experiments, it appears that the encoder embedding has this property under more general models beyond DC-SBM, which warrants further exploration. Extending the definition of this property beyond supervised learning and investigating its finite-sample behavior are also important directions for future research.

References

- [1] M. Girvan and M. E. J. Newman, “Community structure in social and biological networks,” *Proceedings of National Academy of Science*, vol. 99, no. 12, pp. 7821–7826, 2002. 1
- [2] M. E. J. Newman, “The structure and function of complex networks,” *SIAM Review*, vol. 45, no. 2, pp. 167–256, 2003.
- [3] A.-L. Barab’asi and Z. N. Oltvai, “Network biology: Understanding the cell’s functional organization,” *Nature Reviews Genetics*, vol. 5, no. 2, pp. 101–113, 2004.
- [4] S. Boccaletti, V. Latora, Y. Moreno, M. Chavez, and D.-U. Hwang, “Complex networks: Structure and dynamics,” *Physics Reports*, vol. 424, no. 4-5, pp. 175–308, 2006.

- [5] L. Varshney, B. Chen, E. Paniagua, D. Hall, and D. Chklovskii, "Structural properties of the *caenorhabditis elegans* neuronal network," *PLoS Computational Biology*, vol. 7, no. 2, p. e1001066, 2011.
- [6] J. Ugander, B. Karrer, L. Backstrom, and C. Marlow, "The anatomy of the facebook social graph," *arXiv preprint arXiv:1111.4503*, 2011. 1
- [7] K. Rohe, S. Chatterjee, and B. Yu, "Spectral clustering and the high-dimensional stochastic blockmodel," *Annals of Statistics*, vol. 39, no. 4, pp. 1878–1915, 2011. 1
- [8] D. Sussman, M. Tang, D. Fishkind, and C. Priebe, "A consistent adjacency spectral embedding for stochastic blockmodel graphs," *Journal of the American Statistical Association*, vol. 107, no. 499, pp. 1119–1128, 2012. 1, 2
- [9] T. N. Kipf and M. Welling, "Semi-supervised classification with graph convolutional networks," in *International Conference on Learning Representations*, 2017. 1, 2
- [10] Z. Wu, S. Pan, F. Chen, G. Long, C. Zhang, and P. S. Yu, "A comprehensive survey on graph neural networks," *IEEE Transactions on Neural Networks and Learning Systems*, vol. 32, pp. 4–24, 2019. 1
- [11] A. Grover and J. Leskovec, "node2vec: Scalable feature learning for networks," in *Proceedings of the 22nd ACM SIGKDD international conference on Knowledge discovery and data mining*, pp. 855–864, 2016. 1
- [12] R. Liu and A. Krishnan, "Pecanpy: a fast, efficient and parallelized python implementation of node2vec," *Bioinformatics*, vol. 37, no. 19, pp. 3377–3379, 2021. 1
- [13] B. Karrer and M. E. J. Newman, "Stochastic blockmodels and community structure in networks," *Physical Review E*, vol. 83, p. 016107, 2011. 2
- [14] Y. Zhao, E. Levina, and J. Zhu, "Consistency of community detection in networks under degree-corrected stochastic block models," *Annals of Statistics*, vol. 40, no. 4, pp. 2266–2292, 2012. 2, 5
- [15] B. Perozzi, R. Al-Rfou, and S. Skiena, "Deepwalk: Online learning of social representations," in *Proceedings of the 20th ACM SIGKDD international conference on Knowledge discovery and data mining*, pp. 701–710, ACM, 2014. 2

- [16] S. Ranshous, S. Shen, D. Koutra, S. Harenberg, C. Faloutsos, and N. F. Samatova, "Anomaly detection in dynamic networks: a survey," *Wiley Interdisciplinary Reviews: Computational Statistics*, vol. 7, no. 3, pp. 223–247, 2015. 2
- [17] L. Akoglu, H. Tong, and D. Koutra, "Graph based anomaly detection and description: A survey," *Data Mining and Knowledge Discovery*, vol. 29, no. 3, pp. 626–688, 2015. 2
- [18] C. Shen, Q. Wang, and C. E. Priebe, "One-hot graph encoder embedding," *IEEE Transactions on Pattern Analysis and Machine Intelligence*, accepted, 2023. 2, 4, 5, 1
- [19] P. Holland, K. Laskey, and S. Leinhardt, "Stochastic blockmodels: First steps," *Social Networks*, vol. 5, no. 2, pp. 109–137, 1983. 2
- [20] T. Snijders and K. Nowicki, "Estimation and prediction for stochastic blockmodels for graphs with latent block structure," *Journal of Classification*, vol. 14, no. 1, pp. 75–100, 1997. 2
- [21] C. E. Priebe, D. J. Marchette, Z. Ma, and S. Adali, "Manifold matching: Joint optimization of fidelity and commensurability," *Brazilian Journal of Probability and Statistics*, vol. 27, no. 3, pp. 377–400, 2013. 2
- [22] V. Lyzinski, Y. Park, C. E. Priebe, and M. W. Trosset, "Fast embedding for jofc using the raw stress criterion," *Journal of Computational and Graphical Statistics*, vol. 26, no. 4, pp. 786–802, 2017. 2
- [23] J. Arroyo, A. Athreya, J. Cape, G. Chen, C. E. Priebe, and J. T. Vogelstein, "Inference for multiple heterogeneous networks with a common invariant subspace," *Journal of Machine Learning Research*, vol. 22, no. 142, pp. 1–49, 2021. 2
- [24] I. Gallagher, A. Jones, and P. Rubin-Delanchy, "Spectral embedding for dynamic networks with stability guarantees," *Advances in Neural Information Processing Systems*, 2021. 2
- [25] C. Shen, Y. Park, and C. E. Priebe, "Graph encoder ensemble for simultaneous vertex embedding and community detection," <https://arxiv.org/abs/2301.11290>, 2023. 4, 13

- [26] C. Shen, J. Larson, H. Trinh, X. Qin, Y. Park, and C. E. Priebe, “Discovering communication pattern shifts in large-scale networks using encoder embedding and vertex dynamics,” <https://arxiv.org/abs/2109.13098>, 2023. 4
- [27] R. A. Rossi and N. K. Ahmed, “The network data repository with interactive graph analytics and visualization,” in *AAAI*, 2015. 8
- [28] D. Pavlovic, P. Vertes, E. Bullmore, W. Schafer, and T. Nicholas, “Stochastic block-modeling of the modules and core of the caenorhabditis elegans connectome,” *PLoS ONE*, vol. 9, no. 9, p. e97584, 2014. 9
- [29] L. Chen, J. T. Vogelstein, V. Lyzinski, and C. E. Priebe, “A joint graph inference case study: the c.elegans chemical and electrical connectomes,” *Worm*, vol. 5, no. 2, p. 1, 2016. 9
- [30] A. K. McCallum, K. Nigam, J. Rennie, and K. Seymore, “Automating the construction of internet portals with machine learning,” *Information Retrieval*, vol. 3, pp. 127–163, 2000. 9
- [31] C. L. Giles, K. D. Bollacker, and S. Lawrence, “Citeseer: An automatic citation indexing system,” in *Proceedings of the Third ACM Conference on Digital Libraries*, pp. 89–98, 1998. 9
- [32] P. Yanardag and S. Vishwanathan, “Deep graph kernels,” in *KDD 15: Proceedings of the 21th ACM SIGKDD International Conference on Knowledge Discovery and Data Mining*, pp. 1365–1374, 2015. 9
- [33] K. M. Borgwardt, C. S. Ong, S. Schönauer, S. V. N. Vishwanathan, A. J. Smola, and H.-P. Kriegel, “Protein function prediction via graph kernels,” *Bioinformatics*, vol. 21, pp. i47–i56, 2005. 10
- [34] D. Blei, A. Ng, and M. Jordan, “Latent dirichlet allocation,” *Journal of Machine Learning Research*, vol. 3, pp. 993–1022, 2003. 10
- [35] C. Shen and J. T. Vogelstein, “The exact equivalence of distance and kernel methods in hypothesis testing,” *AStA Advances in Statistical Analysis*, vol. 105, no. 3, pp. 385–403, 2021. 10

- [36] C. Shen, M. Sun, M. Tang, and C. E. Priebe, “Generalized canonical correlation analysis for classification,” *Journal of Multivariate Analysis*, vol. 130, pp. 310–322, 2014. 11
- [37] C. Shen, J. T. Vogelstein, and C. Priebe, “Manifold matching using shortest-path distance and joint neighborhood selection,” *Pattern Recognition Letters*, vol. 92, pp. 41–48, 2017. 11
- [38] V. D. Blondel, J. L. Guillaume, R. Lambiotte, and E. Lefebvre, “Fast unfolding of communities in large networks,” *Journal of Statistical Mechanics: Theory and Experiment*, vol. 10008, p. 6, 2008. 13
- [39] V. A. Traag, L. Waltman, and N. J. van Eck, “From louvain to leiden: guaranteeing well-connected communities,” *Scientific Reports*, vol. 9, p. 5233, 2019.
- [40] U. N. Raghavan, R. Albert, and S. Kumara, “Near linear time algorithm to detect community structures in large-scale networks,” *Physical Review E*, vol. 76, no. 3, p. 036106, 2007. 13

Acknowledgment

This work was supported in part by the National Science Foundation HDR TRIPODS 1934979, the National Science Foundation DMS-2113099, and by funding from Microsoft Research.

APPENDIX

A Proof

A.1 Theorem 1

Proof. The convergence theorem in [18] shows the no-normalization embedding for vertex i of class y satisfies

$$\mathbf{Z}_m(i, k) \xrightarrow{n \rightarrow \infty} \mu(k),$$

where $\mu(k) = \theta_i \mathbf{B}(y, k) E(\theta_i)$. After normalization, the degree coefficients cancels out, and the following convergence is observed:

$$\mathbf{Z}_m(i, k) \xrightarrow{n \rightarrow \infty} \frac{\mathbf{B}_m(y, k)}{\|\mathbf{B}_m(y, :)\|_2}.$$

By concatenating each dimension within graph m , we obtain:

$$\|\mathbf{Z}_m(i, :) - \tilde{\mathbf{B}}_m(y, :)\|_2 \xrightarrow{n \rightarrow \infty} 0.$$

Concatenating each embedding into the fusion encoder embedding yields the following convergence:

$$\|\mathbf{Z}(i, \cdot) - \tilde{\mathbf{B}}(y, :)\|_2 \xrightarrow{n \rightarrow \infty} 0$$

where $\tilde{\mathbf{B}}$ is the row concatenation of every $\tilde{\mathbf{B}}_m$. □

A.2 Theorem 2

Proof. First, note that the convergence in Theorem 1 applies to both training vertices and testing vertices, as the same W is utilized, which is based on the labels of the training vertices only. As the number of training vertices approaches infinity, the embedding for a testing vertex of class y equals the embedding for any training vertex of class y .

Thus, the testing vertices can be classified perfectly if and only if $\tilde{\mathbf{B}}(k, :) \neq \tilde{\mathbf{B}}(l, :)$ for all pairs of classes $k \neq l$. This condition holds if and only if every row of $\tilde{\mathbf{B}}$ is unique. □

A.3 Theorem 3

Proof. Let $\tilde{\mathbf{B}}_{\mathbf{G}_1}$ and $\tilde{\mathbf{B}}_{\mathbf{G}_2}$ denote the concatenated block matrix for \mathbf{G}_1 and \mathbf{G}_2 , respectively. Suppose there are M_1 graphs in \mathbf{G}_1 and M_2 graphs in \mathbf{G}_2 . Since $\mathbf{G}_1 \subseteq \mathbf{G}_2$, it suffices to assume that the first $K \times M_1$ submatrix in $\tilde{\mathbf{B}}_{\mathbf{G}_2}$ equals $\tilde{\mathbf{B}}_{\mathbf{G}_1}$.

For every pair of rows $k \neq l$ where $\tilde{\mathbf{B}}_{\mathbf{G}_1}(k, :) \neq \tilde{\mathbf{B}}_{\mathbf{G}_1}(l, :)$, it is always the case that $\tilde{\mathbf{B}}_{\mathbf{G}_2}(k, :) \neq \tilde{\mathbf{B}}_{\mathbf{G}_2}(l, :)$. However, for any $k \neq l$ such that $\tilde{\mathbf{B}}_{\mathbf{G}_1}(k, :) = \tilde{\mathbf{B}}_{\mathbf{G}_1}(l, :)$, they may become distinct in \mathbf{G}_2 . Thus, any class k that can be perfectly distinguished from other classes in \mathbf{G}_1 will also remain perfectly separated from other classes in \mathbf{G}_2 . However, two different classes k and l that coincide in \mathbf{G}_1 may become separable in \mathbf{G}_2 .

According to Theorem 2, training and testing vertices within class k all converge to the k th row of the concatenated block matrix. Therefore, any vertices that are correctly classified in \mathbf{G}_1 will remain correctly classified in \mathbf{G}_2 , while previously misclassified vertices in \mathbf{G}_1 may become correctly classified in \mathbf{G}_2 . Consequently, we can say that $L(g(\mathbf{G}_2)) \leq L(g(\mathbf{G}_1))$ for sufficiently large n . \square

B Additional Experiments

Here we replicate the simulations and experiments for three competitor methods. Unlike the encoder embedding, these approaches require choosing a dimension parameter d , and we test all possible values of d from 1 to 30. Note that for a single graph, these three methods are essentially the same as the adjacency spectral embedding [8].

The Omnibus method [21, 22] creates a large $Mn \times Mn$ matrix by using the input adjacency on the diagonal, and computing the average of two adjacency matrices on the off-diagonal $n \times n$ sub-matrix. The matrix is then projected into an $n \times d$ matrix using spectral embedding via singular value decomposition. Then we use the 5-nearest-neighbor classifier and report the best error for $d = 1, \dots, 30$.

The Multiple adjacency spectral embedding (MASE) [23] carries out individual spectral embeddings for each adjacency matrix, resulting in an $n \times 30$ matrix for each graph. These matrices are then concatenated into an $n \times 30M$ matrix, followed by another SVD to obtain an $n \times d$ matrix. The best 5-nearest-neighbor error is reported for $d = 1, \dots, 30$.

The Unfolded spectral embedding (USE) [24] concatenates all the adjacency matrices into an $n \times Mn$ matrix, followed by SVD to obtain an $n \times Md$ matrix. The best 5-nearest-

neighbor error is reported for $d = 1, \dots, 30$.

The simulation figures (Figure F1, F2, F3) demonstrate that all three methods are capable of improving classification errors when the additional graph contains signal for the labels. Among the three methods, USE performs the best and has a similar error as the encoder embedding in the main paper. However, in simulation 3, all three methods show a significant degradation in error, especially when five independent graphs are included. For the real data experiments presented in the remaining tables, except for the C-elegans data, all three methods exhibit significantly worse actual classification error compared to the encoder embedding and do not demonstrate the synergistic effect observed for the encoder embedding.

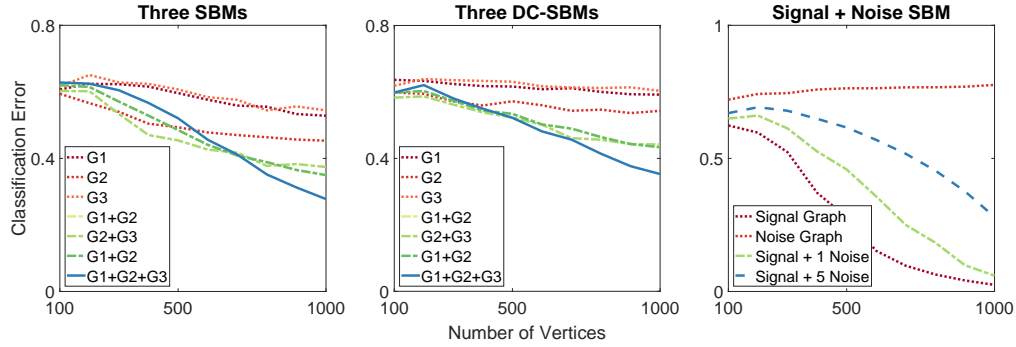


Figure F1: Same experiments as Figure 2 using Omnibus.

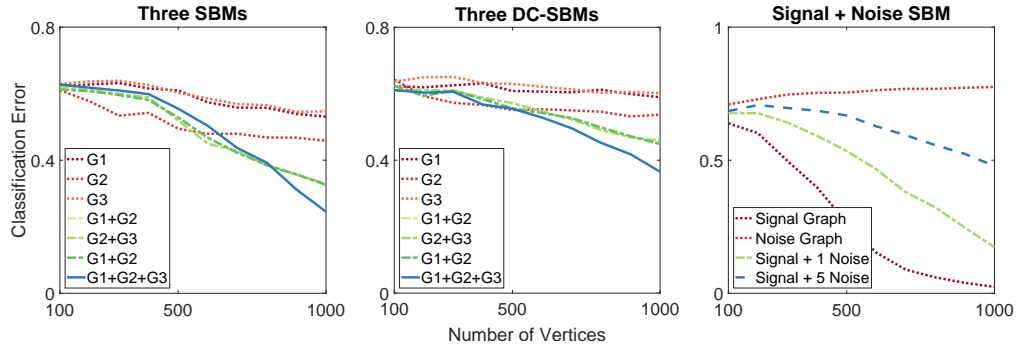


Figure F2: Same experiments as in Figure 2 using MASE.

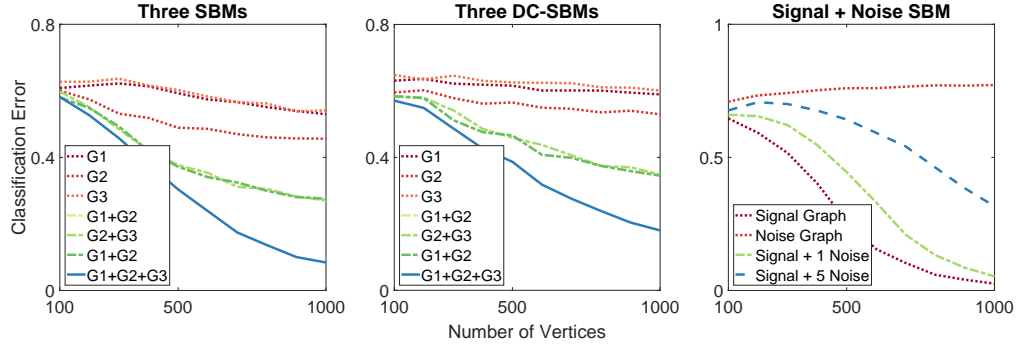


Figure F3: Same experiments as in Figure 2 using USE.

	Graph 1	Graph 2	Graph 1+2
C-elegans	38.7% \pm 1.3%	43.5% \pm 1.2%	35.0% \pm 1.4%
Cora	31.6% \pm 0.72%	41.2% \pm 0.87%	30.7% \pm 0.48%
Citeseer	45.6% \pm 0.69%	37.5% \pm 0.50%	33.7% \pm 0.47%
COIL-RAG	76.2% \pm 0.9%	36.6% \pm 0.5%	23.9% \pm 0.4%
IMDB	19.8% \pm 0.18%	22.2% \pm 0.15%	11.8% \pm 0.15%
Phone	36.5% \pm 0.5%	36.5% \pm 0.5%	36.9% \pm 0.5%
Protein	44.2% \pm 0.9%	35.7% \pm 0.5%	35.8% \pm 0.4%

Table 4: Same evaluation as in Table 1 using Omnibus.

	Graph 1	Graph 2	Graph 1+2
C-elegans	39.0% \pm 1.3%	43.6% \pm 1.3%	33.6% \pm 1.3%
Cora	31.3% \pm 0.41%	41.7% \pm 0.43%	38.2% \pm 0.58%
Citeseer	45.8% \pm 0.39%	37.6% \pm 0.33%	36.6% \pm 0.31%
COIL-RAG	77.5% \pm 0.9%	36.3% \pm 0.5%	23.7% \pm 0.4%
IMDB	19.8% \pm 0.2%	22.2% \pm 0.2%	45.6% \pm 0.2%
Phone	37.3% \pm 0.4%	37.3% \pm 0.4%	37.3% \pm 0.4%
Protein	44.7% \pm 0.9%	35.7% \pm 0.5%	35.7% \pm 0.4%

Table 5: Same evaluation as in Table 1 using MASE.

	Graph 1	Graph 2	Graph 1+2
C-elegans	40.1% \pm 1.5%	44.1% \pm 1.5%	38.2% \pm 1.5%
Cora	31.6% \pm 0.72%	41.2% \pm 0.87%	30.7% \pm 0.48%
Citeseer	46.4% \pm 0.48%	37.3% \pm 0.28%	36.9% \pm 0.32%
COIL-RAG	76.9% \pm 0.9%	35.1% \pm 0.5%	35.0% \pm 0.4%
IMDB	19.8% \pm 0.14%	22.0% \pm 0.25%	12.6% \pm 0.1%
Phone	37.0% \pm 0.4%	37.0% \pm 0.4%	36.4% \pm 0.4%
Protein	44.4% \pm 0.9%	35.3% \pm 0.5%	35.3% \pm 0.4%

Table 6: Same evaluation as in Table 1 using USE.

	English Text	English Hyperlinks	French Text	French Hyperlinks
G₁	21.3% \pm 0.5%	22.3% \pm 0.5%	41.2% \pm 0.7%	45.5% \pm 0.6%
G₂	19.4% \pm 0.4% (1+2)	39.3% \pm 0.6% (3+4)	41.5% \pm 0.6% (1+3)	44.4% \pm 0.5% (2+4)
G₃	34.2% \pm 0.6% (-4)	37.5% \pm 0.6% (-3)	39.7% \pm 0.6% (-2)	39.6% \pm 0.6% (-1)
G₄	36.5% \pm 0.5%			

Table 7: Same evaluation as in Table 3 using Omnibus.

	English Text	English Hyperlinks	French Text	French Hyperlinks
G₁	21.8% \pm 0.4%	23.0% \pm 0.6%	43.5% \pm 0.6%	47.2% \pm 0.5%
G₂	19.0% \pm 0.5% (1+2)	40.8% \pm 0.4% (3+4)	41.3% \pm 0.5% (1+3)	44.2% \pm 0.7% (2+4)
G₃	38.1% \pm 0.7% (-4)	39.9% \pm 0.6% (-3)	39.3% \pm 0.7% (-2)	39.5% \pm 0.6% (-1)
G₄	37.2% \pm 0.5%			

Table 8: Same evaluation as in Table 3 using MASE.

	English Text	English Hyperlinks	French Text	French Hyperlinks
G₁	21.3% ± 0.4%	22.1% ± 0.7%	41.4% ± 0.7%	45.1% ± 0.6%
G₂	19.2% ± 0.4% (1+2)	39.9% ± 0.6% (3+4)	39.9% ± 0.7% (1+3)	43.6% ± 0.6% (2+4)
G₃	38.8% ± 0.8% (-4)	41.3% ± 0.7% (-3)	39.0% ± 0.6% (-2)	39.6% ± 0.6% (-1)
G₄	38.7% ± 0.6%			

Table 9: Same evaluation as in Table 3 using USE.